

PROCEEDINGS OF SPIE

SPIDigitalLibrary.org/conference-proceedings-of-spie

Maunakea Night-Sky Model

Petric, Andreea, Flagey, Nicolas, Marshall, Jennifer,
Barba, Leo, Barden, Samuel, et al.

Andreea O. Petric, Nicolas J. Flagey, Jennifer L. Marshall, Leo Barba, Samuel C. Barden, Alexis Hill, Kei Szeto, Étienne Artigau, Andrew Stephens, "Maunakea Night-Sky Model," Proc. SPIE 11449, Observatory Operations: Strategies, Processes, and Systems VIII, 114491G (15 December 2020); doi: 10.1117/12.2561879

SPIE.

Event: SPIE Astronomical Telescopes + Instrumentation, 2020, Online Only

Maunakea Night-Sky Model

Andreea O. Petric^{*a}, Nicolas J. Flagey^a, Jennifer L. Marshall^b, Leo Barba^b, Samuel C. Barden^c, Alexis Hill^c, Kei Szeto^c, Etienne Artigau^d, Andrew Stephens^e

^a The Space Telescope Science Institute, 3700 San Martin Dr, Baltimore, MD 21218 USA;

^b Mitchell Institute for Fundamental Physics and Astronomy and Department of Physics and Astronomy, Texas A&M University, College Station, TX 77843-4242, ^cThe Maunakea Spectroscopic Explorer Project Office, 65-1238 Mamalahoa Hwy Kamuela, HI

96743 USA, ^dInstitut de Recherche sur les Exoplanetes, Departement de Physique, Universitde de Montreal, C.P. 6128, Succ. Centre-Ville, Montreal, QC, H3C 3J7, Canada, ^eNOIRlab/Gemini Observatories, 670 N A'ohoku Pl, Hilo, HI, 96720, USA

ABSTRACT

Maunakea Spectroscopic Explorer (MSE) is the first of the future generation of massively multiplexed spectroscopic 11.25m mirror facility on a recycled site. MSE is designed to enable transformative science, being completely dedicated to large-scale multi-object spectroscopic surveys, each studying thousands to millions of astrophysical objects. MSE's transformational potential lies in answering numerous scientific questions and finding new puzzles. Its success will depend in part on its ability to detect large populations of faint sources, from those responsible for reionization to merging galaxies at cosmic dawn and the stellar populations of nearby dwarf galaxies. This capability is set, in part, by our ability to remove the sky from the target spectra. Here we describe the initial steps in a three-year long effort to develop a model of the Maunakea skies comparable to the model developed by ESO of the southern ESO sites. The model will be used to derive best-practices (e.g. the number of required fibers given specific observing conditions, and required sensitivity) and sky subtraction algorithms to achieve $\ll 1\%$ sky subtraction accuracy

Keywords: sky-subtraction, NIR spectroscopy, sky background

1. INTRODUCTION

Modern wide-field imaging surveys such as Pan-STARRS (Chambers et al. 2016), the Dark Energy Survey (Dark Energy Survey Collaboration 2018), and eventually the Vera Rubin Observatory's Large Synoptic Survey (VRO; Ivezić et al. 2008) open a new window on the Universe, enabling the discovery and study of stars and galaxies too faint to be studied previously. To realize the full scientific potential of these surveys, we must examine those objects using spectroscopic techniques. The 2010 Decadal Survey of Astronomy produced by the U.S. National Academies identified multi-object spectroscopic instrumentation on large telescopes as an essential capability for investigations into the fundamental nature of our Universe. More recently, in 2015, the National Research Council explicitly emphasized the need to develop new spectroscopic facilities to enhance the scientific return of the VRO project in its report "Optimizing the U.S. Ground-Based Optical and Infrared Astronomy System."

Given the large numbers of objects to be studied – some *individual* science cases require observations of tens of millions of sources – we must develop an efficient process to carry out these

surveys. Several massively multiplexed spectroscopic instruments are currently in the planning phase or nearing execution. The first of these instruments will be installed on modest-sized 4m-class telescopes and, therefore, will primarily study objects that are brighter than the sky background. To analyze the much more numerous, faint objects of interest discovered in modern wide-field imaging surveys such as VRO, massively multiplexed spectrographs must be installed on larger, 10m-class telescopes. The faintest objects will be much fainter than the sky background and will require larger 30m-class telescopes.

Astronomy communities worldwide have expressed a strong desire to obtain access to a large aperture, wide field of view, highly multiplexed, dedicated spectroscopic facility. The Office of Maunakea Management identified the Canada France Hawaii Telescope (CFHT) site as a redevelopment site in the Comprehensive Management Plan. CFHT, thus, proposed to transform its facility into the Maunakea Spectroscopic Explorer (MSE), an observatory unique in its capability to study more than 4,000 astronomical objects at once, in the visible and near-infrared (NIR), with a range of spectral resolutions. MSE is the project that aims at transforming the CFHT, with an expanded partnership including continental U.S. universities and NOAO, into an 11.25-m telescope inside CFHT's current structure. While the primary mirror of CFHT is 3.6 meters in diameter, the entire summit facility can accommodate an 11.25-meter mirror **without changing the observatory's footprint.**

With its 11.25m aperture telescope, a 1.5 square degree field of view, and operations fully dedicated to multi-object spectroscopy, MSE is designed for transformative, high precision studies of faint astrophysical phenomena. More than 3200 fibers will feed spectrographs operating at low ($R \sim 3000$) and moderate ($R \sim 6000$) spectral resolutions, and more than 1000 fibers will feed spectrographs operating at high ($R \sim 20/40K$) resolution. All spectrographs are available all the time. The entire visible window from 360–950 nm and the near-infrared J and H bands will be accessible at the lower resolutions. The windows in the visible range will be available at the highest resolution. The entire MSE system is optimized for high signal-to-noise observations of the faintest sources in the Universe. High-quality calibration and stability are ensured through the observatory's dedicated operational mode, ensuring that more than 10 million fiber hours of 10-m class spectroscopy are available for forefront science every year. **The discovery efficiency of MSE is an order of magnitude higher than any other spectroscopic capability currently realized or in development. It will produce datasets equivalent in the number of objects to an SDSS Legacy Survey every seven weeks, on a telescope with an aperture 20 times larger and at arguably the best astronomical site on the planet.**

2. NEED FOR BETTER THAN 1% SKY SUBTRACTION ACCURACY

Most science cases for MSE will rely on its ability to detect faint sources and/or measure the widths of narrow lines next to skylines. Both capabilities are dependent on our ability to subtract the contribution of the sky to the measured spectra. Several science cases drive the need for better than 1% sky subtraction. Here we focus on high redshift active galactic nuclei (AGN) hosts as an example. To study the hosts of high redshift AGN ($z > 1$), measure the gas's ionization state in their host galaxies, and infer accretion rates and extinction-corrected star formation rates, we need to measure several emission lines with varying ionization potentials. With MSE, we want to count

those lines in faint and obscured AGN (e.g., sources with I.R. luminosities $\sim 10^{11} L_{\odot}$) because those AGN's luminosity functions may differ from those of un-obscured and/or brighter AGN. For this, we will require 1σ sensitivities at $m_{AB} \approx 23-24$ in one hour. Halo occupation and reionization science cases require similar sensitivities. We will also need to build templates by combining hundreds of spectra in bins of luminosity, redshift, stellar-mass, or other photometrically-derived properties. Errors from sky subtraction may induce systematic effects in stacking, especially in the near-infrared.

Uncertain sky subtraction impacts the uncertainty of the spectra extracted from the science targets and affects the final sensitivity achieved. Using typical "dark" time conditions on Maunakea, as-designed low-resolution spectrograph mode of MSE, and exposure times of 15 and 60 minutes, we find that the accuracy required on the sky subtraction shall be at worst 1% in the optical and better than 0.5% in the near-infrared. Figure (left) compares the limiting magnitude of the as-designed low-resolution throughput of MSE with perfect sky subtraction and the noise equivalent magnitude due to non-perfect sky subtraction. There is about one magnitude difference between the noise equivalent magnitude for sky subtraction at the 1% level and the magnitude limit with a signal to noise ratio (SNR) of 1 in the optical range: slightly more than that in the blue, somewhat less than that in the red.

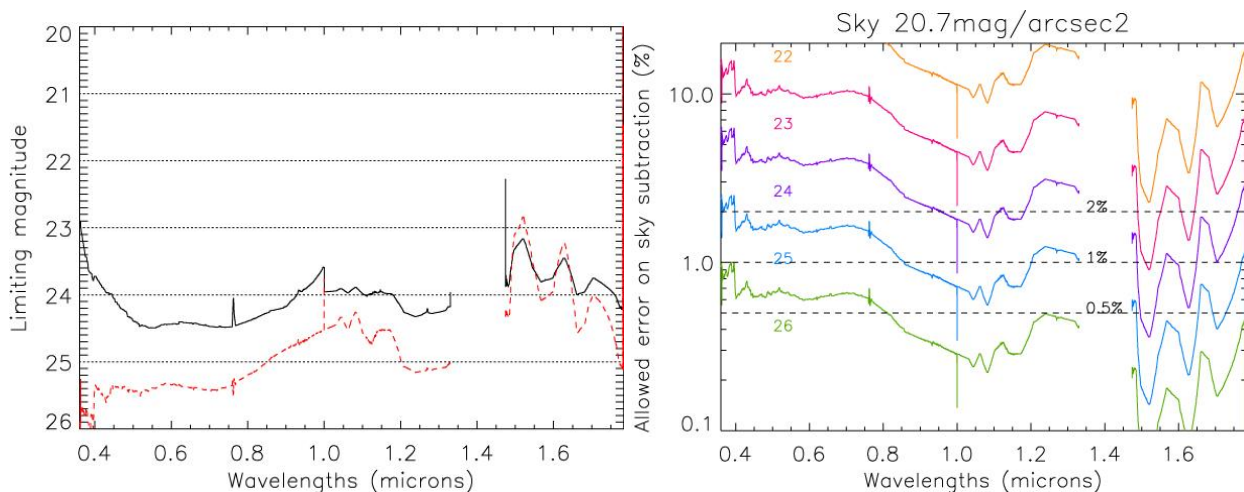


Figure 1: **Left:** limiting magnitudes in the case of a typical "dark" sky brightness of $20.7 \text{ mag/arcsec}^2$, with an error on the sky subtraction of 1%. The limiting magnitude for the whole telescope, assuming perfect sky-subtraction, at $\text{SNR}=1$ is indicated by the solid black line. The noise equivalent magnitude, i.e., the magnitude of a target for which the uncertainty is equal to 1% of the sky emission, is indicated by a red dashed line. **Right:** allowed error on the sky subtraction as a function of wavelength under dark time conditions, for an exposure time of 15 minutes, to obtain a target's spectrum brighter than the noise produced by the poor sky subtraction. The target magnitudes are indicated on the left side.

This means that we will reach the predicted magnitude limits without significantly lowering the SNR if we subtract the sky emission to at least the 1% accuracy level. However, in the near-infrared, both magnitudes are similar, which indicates that the actual SNR on the target's spectrum will be lower than 1 if the sky subtraction is not significantly better than 1%.

Similarly, Figure (right) shows the allowed error on the sky subtraction in typical "dark" sky conditions for different noise equivalent magnitudes between 22 and 26. In the visible, the as-designed throughput of MSE allows observations down to magnitude 24^{th} if the sky subtraction is

good to about 1%. In the near-infrared, the accuracy of the sky subtraction should significantly better than 1% to reach the same survey depth.

Consequently, to make sure we can get a final SNR that is not significantly lower than that expected based on the overall throughput of the telescope with perfect sky subtraction, a sky subtraction accuracy of 1% is a strict minimum in the visible. However, an accuracy of 0.5% is required in the near-infrared.

3. AN ARCHIVE OF OPTICAL-TO-NIR, SKY-SUBTRACTED SPECTRA, A MAUNAKEA SKY MODEL, MSE, AND BEYOND

Our first goal is to develop a sky model similar to the model ESO created for the southern skies at Cerro Paranal and La Silla (e.g., Noll et al. 2012). The ESO sky model includes realistic prescriptions of the sky, including emission, absorption, and scattering associated with the Earth's atmosphere. While the initial motivation was to develop more accurate Exposure Time Calculators, this modeling tool was used to develop a general method for spectroscopic sky subtraction (Noll et al. 2014). An added benefit of the analysis we commenced, beyond MSE, will be a publicly available archive of sky-subtracted optical and NIR spectra obtained with Maunakea telescopes.

We will develop a similar tool for the Maunakea site because its characteristics are much different from the ESO sites. We have compared the magnitudes expected within the H band by the ESO model to those observed on-sky by Gemini¹. For the ESO model, we generate many sky spectra towards multiple sources in the sky (R.A. range from 10° to 298 and DEC range from -26° to +89°). For each source, we generate hundreds of spectra to simulate seasonal variations as well as Moon phases, distances to the Moon, time since sunset, and more. We account for a discrepancy between the ESO and Gemini filters: in the H band, a difference of about 0.11 mag/arcsec² is measured, with the Gemini filter leading to slightly brighter measurements than the ESO filter, while in the J band, using the Gemini filter leads to measurements of the sky brightness ~0.4 mag/arcsec² brighter than using the ESO filter. The comparison between predicted sky brightness and observed sky brightness then reveals the following. We find a discrepancy of a few 0.1 mag/arcsec² in the H band between the ESO simulations and the Gemini observations. The ESO SkyCalc model leads to a slightly fainter night sky than observed by Gemini. The difference between the magnitudes measured using ESO and Gemini filters mentioned earlier might be enough to explain this discrepancy. In the J band, the discrepancy seems significantly larger (0.5 to 1.0 mag/arcsec²), and the difference due to the filters explains only about 0.4 mag/arcsec² of the difference. **Given the importance of accurately subtracting the sky from the MSE observations, we need to characterize the sky emission to better than a few 0.1 mag/arcsec² across the offered spectral range.** Therefore, using the ESO SkyCalc model is not an option, and developing a model for Maunakea will be the first objective in our project.

Our goal is to derive observational best practices – numbers of required sky fibers, exposure times appropriate for the observing conditions – and employ sky subtraction methods to achieve 0.5-1% sky subtraction accuracy in the visible to near-IR for fiber-fed spectrographs on large aperture telescope. We summarize the steps we envisioned in this project in Figure 2: (1) we gather relevant

¹ <https://ui.adsabs.harvard.edu/abs/2016SPIE.9910E..1BR/abstract>

data, (2) we reduce spectra and images, (3) we measure relevant parameters and correlate with observing conditions, (4) we derive a sky model, (5) we establish the best strategy and method to subtract the sky emission and apply it on archived spectra.

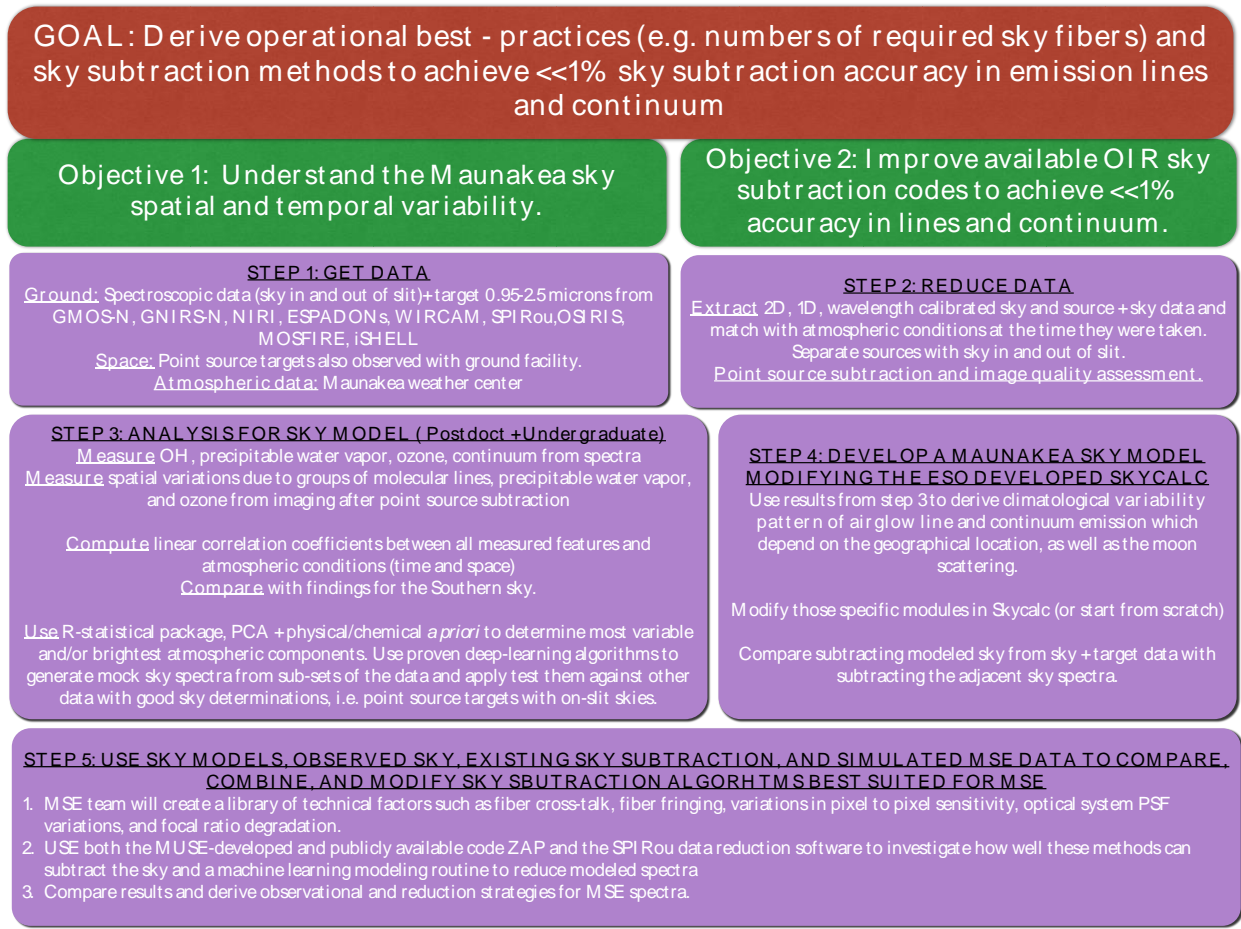


Figure 2: the steps we will take in the proposed project.

4. A FIRST LOOK AT TEMPORAL VARIATIONS OF SKY LINES FROM HIGH RESOLUTION NIR SPECTRA

During December 2018-Jan 2019 the CFHT hydraulics broke which did not allow normal observations. Because the superb near-infrared spectropolarimeter and high precision velocimeter SPIRou (e.g. Moutou et al. 2015) was on the telescope we decided to observe the night sky in 5-10 minutes integrations to estimate temporal variations in the night sky lines. A full analysis will be published in Barba et al. Here we show a few preliminary results.

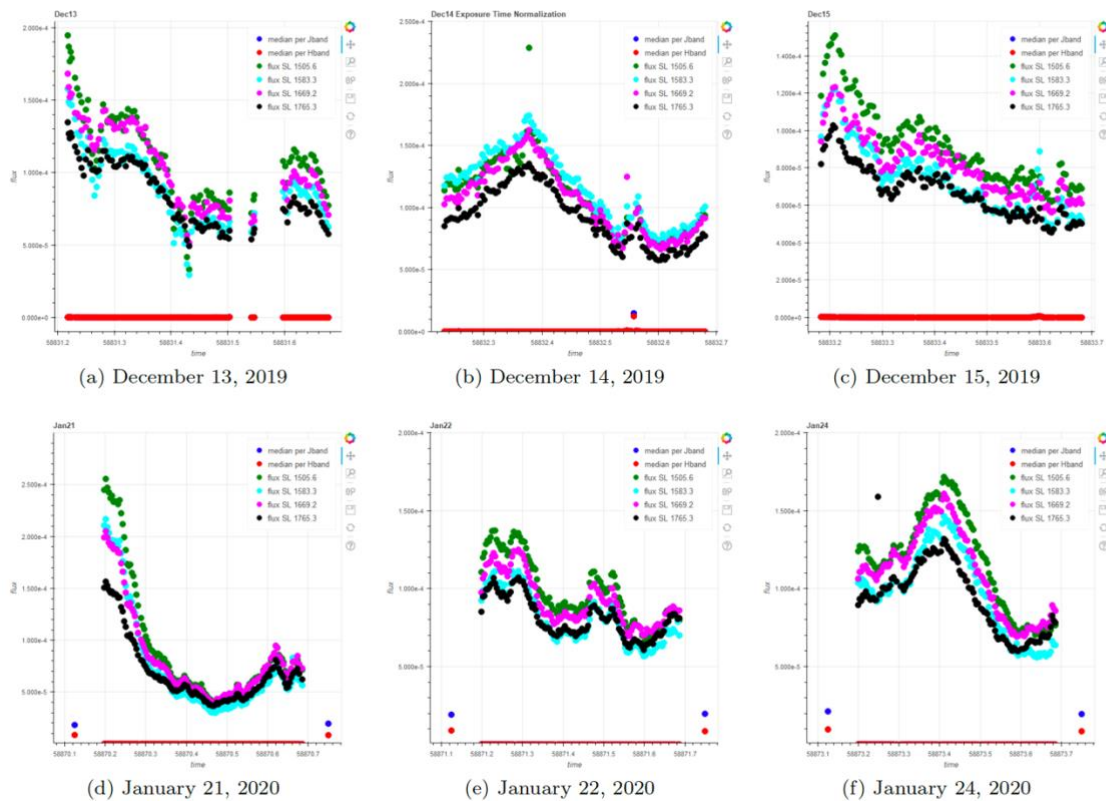


Figure 3: Flux as a function of time for each of the six night of SPIRou sky observations.

5. CONCLUSIONS AND FUTURE WORK

Machine learning techniques have gained traction within the astronomy community (see Ntampaka et al. 2019 for an overview). Deep learning is a powerful, efficient method to extract subtle signals from data by processing the data through multiple unseen layers (e.g., LeCun et al. 1999). Autoencoders (Rumelhart, Hinton, and Williams 1986) are a class of deep learning algorithms that have been applied in astronomy for a range of tasks, including generating realistic galaxy images (Ravanbakhsh et al. 2016), classifying supernovae (Villar et al. 2020), and extracting new physical information from catalogs (Ntampaka & Vikhlinin, 2020, in prep.). A traditional application of an autoencoder can be thought of as a flexible version of principal component analysis, summarizing a complicated signal in a few essential values and then reconstructing the input signal. Because autoencoders build both a flexible compression ("encoder") and decompression ("decoder") of data, they can be used as both a replacement for PCA and also as a data generation tool. This research will explore the use of decoders for quickly generating many realistic mock sky spectra. We will make all codes, models, and strategies with descriptions of the modifications available to the community.

Assuming the best sky subtraction can be performed with slit spectra, a first series of tests of the model and derived algorithms will be executed on real slit spectrograph data. This will establish a baseline for sky subtraction accuracy in ideal conditions where the sky emission is measured simultaneously and almost at the same location as the target.

Then, to thoroughly test sky subtraction strategies and algorithms, we will first need a complete end-to-end simulator for MSE that includes all the instrumental effects (e.g., all the fiber-related impacts) and generates spectra on the spectrographs' detectors. The simulator will be modular to be upgraded when a better understanding of instrumental effects is reached. We will use the Maunakea Sky Model as an input to the simulator to generate observed sky spectra, taking into account spatial and temporal variabilities. We will apply sky subtraction algorithms in various conditions (number and separation of sky fibers) to test whether the simulated sky spectra can be modeled to a 0.5% precision level when the fibers are not "contaminated" by the spectrum of a star/galaxy. We will use the algorithms listed above and others that may come online in the next three years. We will implement additional features, including *a priori* conditions on the decomposition of the sky spectra based on our knowledge of the Maunakea sky emission components and their variabilities. Adding star/galaxy spectra to the simulator's input will then test the sky subtraction algorithms and strategies in real conditions when the sky spectra are "contaminated" with a non-sky component. We will make all our results, data products, and codes available on the MSE webpage. **This work will benefit the MSE community and many other projects associated with the Maunakea Observatories and other projects with fiber-fed spectrographs.**

*apetric@stsci.edu,

petric@mse.cfht.hawaii.edu

REFERENCES

Étienne Artigau, Nicola Astudillo-Defru, Xavier Delfosse, François Bouchy, Xavier Bonfils, Christophe Lovis, Francesco Pepe, Claire Moutou, Jean-François Donati, René Doyon, Lison Malo, 2014, SPIE, 914905

Bertin, E., & Arnauts, S., 1996, A&AS, 117, 393

Davies, R., 2007, MNRAS 375, 1099

Drinkwater, Michael J.; Jurek, Russell J.; Blake, Chris; Woods, David; Pimblet, Kevin A.; Glazebrook, Karl; Sharp, Rob; Pracy, Michael B.; Brough, Sarah; Colless, Matthew; Couch, Warrick J.; Croom, Scott M.; Davis, Tamara M.; Forbes, Duncan; Forster, Karl; Gilbank, David G.; Gladders, Michael; Jelliffe, Ben; Jones, Nick; Li, I. -Hui Madore, Barry; Martin, D. Christopher; Poole, Gregory B.; Small, Todd; Wisnioski, Emily; Wyder, Ted; Yee, H. K. C. 2010, MNRAS, 401, 1429

Ellis, S., C., & Blandford, J., 2008, MNRAS, 386, 47

Hopkins, A., McClure-Griffiths, & Gaensler, 2008, ApJL, 682, L13

- Jones, A., Noll, S.; Kausch, W.; Szyszka, C.; Kimeswenger, S. et al. 2013, *A&A*, 560, A91
- Kausch, W., Noll, S.; Smette, A.; Kimeswenger, S.; Barden, M.; Szyszka, C.; Jones, A. M.; Sana, H.; Horst, H.; Kerber, F., 2015, *A&A*, 576, 78
- Kausch, W., Kondrak, M.; Noll, S.; Lakićević, M.; Kimeswenger, S.; Przybilla, N.; Unterguggenberger, S.; Leschinski, K.; Czoske, O.; Zeilinger, W. 2017, *Astronomical Data Analysis Software and Systems XXV*, ASP, Conference Series, Vol 512, 531
- Lakicevic, M., Kimeswenger, Stefan; Noll, Stefan; Kausch, Wolfgang; Unterguggenberger, Stefanie; Kerber, Florian. 2016, *A&A*, 588, A32
- Maihara, Toshinori; Iwamuro, Fumihide; Yamashita, Takuya; Hall, Donald N. B.; Cowie, Lennox L.; Tokunaga, Alan T.; Pickles, Andrew, 1993, *PASP*, 105, 940
- Marziani, P.; Dultzin-Hacyan, D.; D'Onofrio, M.; Sulentic, J. W. 2003, *AJ*, 125, 1897
- Moehler, S.; Modigliani, A.; Freudling, W.; Giammichele, N.; Gianninas, A.; Gonneau, A.; Kausch, W.; Lançon, A.; Noll, S.; Rauch, T.; Vinther, J. 2014, *A&A*, 568
- Noll, S.; Kausch, W.; Barden, M.; Jones, A. M.; Szyszka, C.; Kimeswenger, S.; Vinther, J. 2012, *A&A*, 543, A92
- LeCun Y., Haffner P., Bottou L., Bengio Y. (1999) Object Recognition with Gradient-Based Learning. In: *Shape, Contour and Grouping in Computer Vision. Lecture Notes in Computer Science*, vol 1681. Springer, Berlin, Heidelberg. https://doi.org/10.1007/3-540-46805-6_19
- Noll, S.; Kausch, W.; Kimeswenger, S.; Barden, M.; Jones, A. M.; Modigliani, A.; Szyszka, C.; Taylor, J. 2014, *A&A*, 567, A25
- Noll, S.; Kausch, W.; Kimeswenger, S.; Unterguggenberger, S.; Jones, A. M. 2015, *Atmos. Chem. Phys.*, 15, 3647
- Noll, Stefan; Kausch, Wolfgang; Kimeswenger, Stefan; Unterguggenberger, Stefanie; Jones, Amy M. 2016, *Atmos. Chem. Phys.* 16, 5021
- Ntampaka, Michelle, Avestruz, Camille; Boada, Steven, Joao Caldeira, Jessi Cisewski-Kehe, Rosanne Di Stefano, Cora Dvorkin, August E. Evrard, Arya Farahi, Doug Finkbeiner, Shy Genel, Alyssa Goodman, Andy Goulding, Shirley Ho, Arthur Kosowsky, Paul La Plante, François Lanusse, Michelle Lochner, Rachel Mandelbaum, Daisuke Nagai, Jeffrey A. Newman, Brian Nord, J. E. G. Peek, Austin Peel, Barnabas Poczós, Markus Michael Rau, Aneta Siemiginowska, Dougal J. Sutherland, Hy Trac, Benjamin Wandelt, 2019, *Astro2020: Decadal Survey on Astronomy and Astrophysics*, science white papers, no. 14; *Bulletin of the American Astronomical Society*, Vol. 51, Issue 3, id. 14

Patat F. 2008, A&A, 481, 575

Parry, I. R., & Carrasco, E., 1990, SPIE, 19133

Puech, M.; Rodrigues, M.; Yang, Y.; Flores, H.; Royer, F.; Disseau, K.; Gonçalves, T.; Hammer, F.; Cirasuolo, M.; Evans, C. J.; Li Causi, G.; Maiolino, R.; Melo, C. 2014 SPIE, 9147

Ravanbakhsh, S.; Lanusse, F.; Mandelbaum, R.; Schneider, R.; Poczós, P., 2016 arXiv 160905796R

Rodrigues, M.; Flores, H.; Puech, M.; Yang, Y.; Royer, F. 2010, SPIE, 77356

Rousselot, P.; Lidman, C.; Cuby, J. -G.; Moreels, G.; Monnet, G. 2000, A&A, 354, 1134

dos Santos, Jesulino Bispo; de Oliveira, Antonio Cesar; Gunn, James; de Oliveira, Ligia Souza; Vital de Arruda, Marcio; Castilho, Bruno; Gneiding, Clemens Darwin; Ribeiro, Flavio Felipe; Murray, Graham; Reiley, Daniel J.; Sodr  Junior, Laerte; de Oliveira, Claudia Mendes 2014, SPIE, 2056460

Sharp, R., & Parkinson, H., 2010, MNRAS, 408, 2495

Smette, A.; Sana, H.; Noll, S.; Horst, H.; Kausch, W.; Kimeswenger, S.; Barden, M.; Szyszka, C.;

Jones, A. M.; Gallenne, A.; Vinther, J.; Ballester, P.; Taylor, J. 2015, A&A, 576, 77S

Soto, Kurt T.; Lilly, Simon J.; Bacon, Roland; Richard, Johan; Conseil, Simon 2016, MNRAS, 458, 3210

Rumelhart, D., Hinton, G. & Williams, R. Learning representations by back-propagating errors. *Nature* **323**, 533–536 (1986). <https://doi.org/10.1038/323533a0>

Villar, V. Ashley; Hosseinzadeh, Griffin; Berger, Edo; Ntampaka, Michelle; 2020, ApJ, submitted, eprint arXiv:2008.04921

Wild, V & Hewet, P., MNRAS, 358, 1083

Yang, Y.; Rodrigues, M.; Puech, M.; Flores, H.; Royer, F.; Disseau, K.; Gonçalves, T.; Hammer, F.; Cirasuolo, M.; Evans, C.; Li Causi, G.; Maiolino, R.; Melo, C., 2013, ESO Messenger, March 2013

Zhang, B., Zhang, L., & Ye, Z., 2016, PASA, 33, E058 Zhu., J., & Ye, Z., 2012, PASA, 29